The Hitchhiker's Guide to Particle Flow-Based Filters: A Survey

Sukkeun Kim * **Uwe D. Hanebeck** *

* *Intelligent Sensor-Actuator-Systems Laboratory (ISAS), Institute for Anthropomatics and Robotics Karlsruhe Institute of Technology (KIT), 76131 Karlsruhe, Germany (e-mail: sukkeun.kim@kit.edu; uwe.hanebeck@kit.edu).*

Abstract: Particle flow-based filters migrate samples toward the posterior, instead of using importance weighting, to mitigate the particle degeneracy issue in particle filters. Although a large number of related studies exist, the absence of a survey makes it difficult to follow the current developments. This study aims to survey particle flow-based filters and provide a guide with numerical examples for those who are new to these filters. We survey three main branches of studies that employ the idea of particle flows in the measurement update step. The main algorithms from the three branches are compared with extensive analysis using numerical examples, highlighting their relative performance characteristics and practical considerations.

Keywords: Estimation and filtering, Filtering and smoothing, Kalman filtering, Stochastic control, Stochastic differential equations.

1. INTRODUCTION

Particle flow-based filters are estimation algorithms that migrate samples toward the posterior to mitigate the particle degeneracy issue in particle filters (PFs). This issue often occurs with a high signal-to-noise ratio (SNR) measurement or when the overlap between the likelihood and the prior density is very small (Daum and Huang, 2011a). The particle degeneracy issue is a critical challenge to the performance of PFs since the number of effective particles decreases, and the remaining particles are no longer able to represent the posterior density adequately (Li et al., 2014). To alleviate this issue, many approaches have been proposed. One of the most straightforward approaches is resampling (Li et al., 2014, 2015a; Kuptametee and Aunsri, 2022) where new particles are sampled from the ones with large weights, and Gaussian mixtures (GMs) are also utilised to approximate the posterior density to overcome this issue (Kotecha and Djurić, 2003; Psiaki, 2015; Raihan and Chakravorty, 2018; Kim et al., 2025a, 2026). Recently, many researchers have proposed learning- or artificial intelligence (AI)-based approaches to mitigate this issue (Kim et al., 2022, 2025b).

An alternative approach to alleviating the aforementioned issue is particle flow-based filters. The main idea is migrating the particles with continuous progressive inclusion of the measurement (or homotopy), as shown in Fig. 1, or a discrete control input. Progressive inclusion was introduced in (Oudjane and Musso, 2000; Hanebeck et al., 2003; Hanebeck and Feiermann, 2003), and flow-based filters with log-homotopy were introduced in (Daum and Huang, 2007, 2008, 2009). Homotopy here refers to a continuous transformation between continuous functions rather than simple multiplication in Bayes' rule. They are powerful and efficient for nonlinear and for high-dimensional cases where a large number of particles are required.

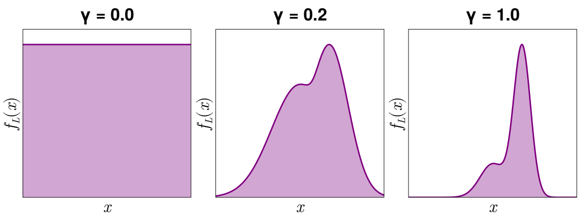

Fig. 1. **Overview of homotopy.** At the initial artificial time $\gamma = 0.0$, no information is included; at $\gamma = 0.2$, information is partially included; and at the final artificial time $\gamma = 1.0$, all information is included. Note that values are not normalised for better visibility.

A plethora of approaches has been proposed over the past decades within this field, but the absence of a survey makes the entry barrier higher and causes hitchhikers to get lost in the galaxy of particle flow-based filters! In this survey, we provide a guide to this galaxy – where to start, where to navigate, and some shortcuts for your pleasant journey. The main contributions of this study are listed as follows:

1) A brief history and evolution of particle flow-based filters are presented.
2) A comprehensive survey of the three main branches, including key papers, is provided.
3) A simulation study of main algorithms, with insights into particle flow-based filters, is provided.

The rest of this study is composed as follows: Section 2 formulates the dynamic system we are interested in. Section 3 introduces the three main groups of particle flow-based filters, and Section 4 presents comparative simulation results of the main algorithms. Section 5 discusses the characteristics and properties of the approaches from each group. Finally, we conclude this study with future work in Section 6. Please fasten your seatbelt!

2. PROBLEM FORMULATION

In a discrete-time dynamic system, a random N-dimensional state vector at time step k, $\underline{\boldsymbol{x}}_k \in \mathbb{R}^N$, can be mapped using the deterministic mapping function $\underline{a}_k$ as shown in (1) [1] :

$$\underline{\boldsymbol{x}}_{k+1} = \underline{a}_k\left(\underline{\boldsymbol{x}}_k, \underline{u}_k, \underline{\boldsymbol{w}}_k\right), \tag{1}$$

where $\underline{u}_k$ is a control input and $\underline{\boldsymbol{w}}_k$ is the system noise. In addition to that, the relationship between the predicted measurement vector $\underline{\boldsymbol{y}}_k$, and the hidden state, $\underline{\boldsymbol{x}}_k$, can be mapped using the deterministic measurement function $\underline{h}_k$ as shown in (2):

$$\underline{\boldsymbol{y}}_k = \underline{h}_k\left(\underline{\boldsymbol{x}}_k, \underline{\boldsymbol{v}}_k\right) \ , \tag{2}$$

where $\underline{\boldsymbol{v}}_k$ is the measurement noise. In the measurement update step, the state is estimated using Bayes' rule once the measurement $\underline{z}_k$ has been observed, as follows:

$$f_k\left(\underline{x}_k|\mathbf{Z}_k\right) \propto f_k\left(\underline{z}_k|\underline{x}_k\right) \cdot f_k\left(\underline{x}_k|\mathbf{Z}_{k-1}\right) \ , \tag{3}$$

where $f_k(\underline{x}_k|\mathbf{Z}_k)$ is the posterior density of the state given the sequence of measurements $\mathbf{Z}_k = \{\underline{z}_1, \underline{z}_2, \ldots, \underline{z}_k\}$, $f_k(\underline{z}_k|\underline{x}_k)$ is the likelihood function f_k^L, associated with actual measurement $\underline{z}_k$, and $f_k(\underline{x}_k|\mathbf{Z}_{k-1})$ is the prior density of the state. In this study, we focus on a single measurement update step with Gaussian additive noise, and (2) can then be simplified by omitting the time step index k as follows:

$$\underline{\boldsymbol{y}} = \underline{h}\left(\underline{\boldsymbol{x}}\right) + \underline{\boldsymbol{v}} \ , \tag{4}$$

where $\underline{\boldsymbol{v}} \sim \mathcal{N}(\underline{0}, \underline{\sigma}_v^2)$ is zero-mean Gaussian noise with standard deviation $\underline{\sigma}_v$, and the estimated density can be simplified as follows:

$$f_e\left(\underline{x}\right) \propto f_L\left(\underline{x}\right) \cdot f_p\left(\underline{x}\right) \ , \tag{5}$$

where $f_e(\underline{x})$, $f_L(\underline{x})$, and $f_p(\underline{x})$ denote posterior density, likelihood function, and prior density, respectively.

3. PARTICLE FLOW-BASED FILTERS

The key idea of particle flow-based filters is to migrate the particles toward the posterior and this can be achieved in two distinct ways. One approach is to apply a small trick in (5), particularly in the likelihood function $f_L(\underline{x})$, so that the measurement can be progressively included in the system using homotopy (or log-homotopy). Another approach is to design the control input $\underline{u}_k$ in (1).

Various approaches employing the aforementioned techniques have been proposed, and most of them are rooted in three main branches from four distinct research groups – Hanebeck's group, Daum's group (Coates' group), and Mehta's group. Each group has been developing its own approach independently, except Coates' group, whose approaches are rooted in Daum's group. The first flow-based filter was proposed by Hanebeck's group in 2003 (Hanebeck et al., 2003), but it was designed for continuous densities, whereas the first particle flow based on log-homotopy was proposed by Daum's group in 2007 (Daum and Huang, 2007). In this section, we review the approaches under the three main branches – progressive Bayesian filters (PBFs) branch in Section 3.1, Daum–Huang filters (DHFs) branch in Section 3.2, and feedback particle filters (FPFs) branch in Section 3.3.

[1] Underlines denote vectors, small boldface indicates random variables and capital boldface indicates matrices. The subscripts p and e denote the predicted and estimated states, respectively.

3.1 Progressive Bayesian Filters Branch

This branch has been driven mainly by Hanebeck's group and is one of the first branches to propose the progressive inclusion of the measurement. The branch is named *Progressive Bayesian Filters Branch* since the first sample-based progressive filters developed within this branch were called progressive Gaussian filters (PGFs). In this survey, we refer to it as progressive Bayesian filters (PBFs).

The progressive inclusion of the measurement can be enabled using artificial time (or homotopy parameter), defined as $\gamma \in [0, 1]$ in the original papers, to construct the homotopy equation from (5) as

$$f_e\left(\underline{x}, \gamma\right) \propto f_L\left(\underline{x}\right)^{\gamma} \cdot f_p\left(\underline{x}\right) \ . \tag{6}$$

From (6) and as shown in Fig. 1, when $\gamma = 0.0$, no measurement is taken into account, and the posterior density is the same as the prior density; when $\gamma = 1.0$, we retrieve the exact posterior based on Bayes' rule. A similar idea was first introduced to filtering by Oudjane and Musso in (Oudjane and Musso, 2000), but this approach suggests dividing the measurement update step, or correction step, into multiple sub-correction steps instead of using homotopy or log-homotopy. Hanebeck et al. proposed a progressive measurement inclusion for GM density formulation in (Hanebeck et al., 2003; Hanebeck and Feiermann, 2003). However, they did not utilise particles, or Dirac mixture approximation (DMA) (Hanebeck et al., 2009), but applied progressive inclusion of the measurement to continuous densities. Another interesting approach is proposed by Hagmar et al. in (Hagmar et al., 2011); however, this approach has not considered the flow of particles either.

Other approaches that utilise the homotopy in (6) and the DMA were proposed later in (Ruoff et al., 2011; Hanebeck and Steinbring, 2012; Hanebeck, 2013), and were named PGFs. The first PGF in (Hanebeck and Steinbring, 2012) is based on moment matching, approximating the Gaussian posterior density by matching the first and second moments of the samples, where the measurement was gradually taken into account in the intermediate Gaussian density. The key elements of another approach (Ruoff et al., 2011) and PGF 42 (Hanebeck, 2013) are the generalised Cramér–von Mises distance (CvMD) based on localised cumulative distribution (LCD) defined in (Hanebeck and Klumpp, 2008), and deterministic DMA based on the generalised CvMD (Hanebeck et al., 2009). PGF 42 minimises the generalised CvMD between an intermediate posterior density approximated by DMA and the posterior density, also approximated by DMA during its measurement update, without an explicit likelihood function. This minimisation yields a continuous ordinary differential equation (ODE), which governs the migration of the particles toward the posterior. This marks the main differences from other particle flow-based approaches: 1) deterministic samples and 2) a distance measure. Further developments in PBFs were proposed later, including the PGF with explicit likelihood (Steinbring and Hanebeck, 2014), the up-sampling progressive Bayesian filter (UsPBF) (Hanebeck and Pander, 2016), and the PGF with a predictor–corrector structure using importance sampling (Chlebek et al., 2016). However, we omit them in this survey due to space limitations and will discuss them in future work.

Instead, we introduce the latest advance of the PBFs, named the Newton-flow (NF) particle filter (Hanebeck, 2025). The NF is similar to PGF 42 but distinct in two main respects: 1) PGF 42 assumes that the intermediate posterior density is Gaussian, whereas NF does not assume any specific form, and 2) NF utilises infinitesimal steps of the flow to ensure the approximated density remains within the permissible space during the measurement update step with homotopy. The NF utilises a reference density $\tilde{f}_e(\underline{x},\gamma)$, which depends on the artificial time γ for the infinitesimal steps, is not limited to any specific density such as a Gaussian. Plugging the reference density $\tilde{f}_e(\underline{x},\gamma)$ into (6) yields

$$\tilde{f}_e\left(\underline{x},\gamma\right) \propto f_L\left(\underline{x}\right)^{\gamma} \cdot f_p\left(\underline{x}\right) \tag{7}$$

and the generalised CvMD between (7) and the true posterior density $f_e(\underline{x},\underline{\eta}(\gamma))$ parametrised with $\underline{\eta}(\gamma)$ can be denoted as

$$D\left(\underline{\eta}\left(\gamma\right),\gamma\right) = D\left(\tilde{f}_e\left(\underline{x},\gamma\right), f_e\left(\underline{x},\underline{\eta}\left(\gamma\right)\right)\right) \ . \tag{8}$$

It is worth noting that the above densities are assumed by the deterministic DMA. In order to obtain the change of the parameter of the posterior density, $\underline{\eta}(\gamma)$, we first take the partial derivative of the distance $D(\underline{\eta}(\gamma),\gamma)$ with respect to the parameter $\underline{\eta}(\gamma)$ and set it to zero. This yields the gradient $\underline{G}\left(\underline{\eta}(\gamma),\gamma\right)$ as

$$\underline{G}\left(\underline{\eta}\left(\gamma\right),\gamma\right) = \frac{\partial D\left(\underline{\eta}\left(\gamma\right),\gamma\right)}{\partial \underline{\eta}\left(\gamma\right)} = 0 \ . \tag{9}$$

Another partial derivative with respect to γ yields the change of the parameter of the posterior density, $\underline{\eta}(\gamma)$, with respect to γ, as

$$\dot{\underline{\eta}}\left(\gamma\right) = -\mathbf{H}^{-1}\left(\underline{\eta}\left(\gamma\right),\gamma\right) \cdot \underline{J}\left(\underline{\eta}\left(\gamma\right),\gamma\right) \ , \tag{10}$$

where $\mathbf{H}$ is a Hessian matrix, which gives the flow its name, "Newton-flow", and $\underline{J}$ denotes the derivative of the gradient vector with respect to γ. The NF assumes infinitesimal steps, and by substituting the reference density with the best approximation density in the next infinitesimal step, the true posterior density is no longer required to solve the ODE in (10). Finally, the NF moves the particles from the prior to the posterior smoothly over the artificial time γ. The NF requires only the prior and the likelihood function, which makes it efficient and versatile in many applications. Further details of the NF can be found in (Hanebeck, 2025). The NF will be considered for the comparative numerical study in Section 4, and further discussion will be provided in Section 5.

We carefully selected the following papers, which contain the key approaches of this branch, for readers:

1) (Hanebeck and Klumpp, 2008): Proposition of LCD and generalised CvMD.
2) (Hanebeck and Steinbring, 2012): PGF based on moment matching – the first PGF presented.
3) (Hanebeck, 2013): PGF 42 based on generalised CvMD and DMA – a powerful filtering approach that does not require the likelihood function.
4) (Hanebeck, 2025): Newton-flow filter based on generalised CvMD and DMA – a simple and efficient filtering approach that requires only the prior and likelihood function.

3.2 Daum–Huang Filters Branch

This branch has been driven mainly by Daum's group and is based on log-homotopy. The terminology "particle flow" for filtering was first introduced in this branch, analogous to its usage in physics. The branch is named *Daum–Huang Filters Branch* after the two main authors of the approaches, and it is later referred to as Daum–Huang filters (DHFs) by other researchers. Based on DHFs, Coates' group also proposed multiple algorithms, including particle flow particle filters (PFPFs), which can be seen as a sub-branch of the DHFs branch.

In DHFs, a log-homotopy, a logarithmic form of the homotopy in (6), was utilised to induce a particle flow, and it was in fact proposed earlier than the PBFs branch. The log-homotopy uses artificial time (or homotopy parameter), originally defined as $\lambda \in [0,1]$ in the original papers. For clarity, we shall use the same notation as in (6), and it is defined as follows:

$$\log f_e\left(\underline{x},\gamma\right) = \log f_p\left(\underline{x}\right) + \gamma \log f_L\left(\underline{x}\right) - \log \kappa\left(\gamma\right) \ , \tag{11}$$

where $\kappa(\gamma)$ is the normalising term in Bayes' rule. This log-homotopy was first proposed for filtering by Daum and Huang in (Daum and Huang, 2007, 2008), and the complete form of the filter was presented in (Daum and Huang, 2009). The particle flow is induced as a partial differential equation (PDE) derived from the log-homotopy by taking the partial derivative of the log-homotopy with respect to the artificial time γ. The general solution of the particle flow $g_f(\underline{x},\gamma)$ can be obtained as follows:

$$\begin{aligned} g_f\left(\underline{x},\gamma\right) &= \frac{d\underline{x}}{d\gamma} \\ &= -\mathbf{C}^{\#}\frac{\partial \log f_e(\underline{x},\gamma)}{\partial \gamma} + \left[\mathbf{I} - \mathbf{C}^{\top}\mathbf{C}/\mathrm{tr}\left(\mathbf{C}^{\top}\mathbf{C}\right)\right]\underline{c} \ , \end{aligned} \tag{12}$$

$$\mathbf{C} = \frac{\partial \log f_e\left(\underline{x},\gamma\right)}{\partial \underline{x}} \ , \tag{13}$$

where $\mathbf{C}^{\#}$ is the generalised inverse of $\mathbf{C}$ and $\underline{c}$ is an arbitrary vector. Further details of the derivation can be found in (Daum and Huang, 2009). The first works are later referred to as "incompressible flow" by the authors due to their incompressible assumption, $\nabla \cdot g_f(\underline{x},\gamma) = 0$, which leads to an approximate flow. The terminology is borrowed from fluid dynamics, where the divergence of the flow velocity is assumed to be zero (as in subsonic flight in air). In the actual implementation, the key part of the algorithm is the approximation of the gradient of the log-prior density, $\log f_p\left(\underline{x}\right)$, in

$$\frac{\partial \log f_e\left(\underline{x},\gamma\right)}{\partial \underline{x}} = \frac{\partial \log f_p\left(\underline{x}\right)}{\partial \underline{x}} + \gamma\frac{\partial \log f_L\left(\underline{x}\right)}{\partial \underline{x}} \ , \tag{14}$$

and multiple approaches to approximating this gradient were proposed in (Daum et al., 2009a,b). It is worth noting that the normalisation term, $\kappa(\gamma)$, in the log-homotopy in (11) was not considered in the initial papers, appearing only in later developments.

Chen and Mehra (Chen and Mehra, 2010) examined the incompressible flow and suggested that a singularity, caused by the denominator of the flow becoming zero, can occur in one-dimensional nonlinear filters under certain initial conditions. In addition, they pointed out this can result in the non-existence of the flow and further proposed some workarounds to overcome this issue. Daum and Huang, however, responded that it is avoidable if the dimension is higher than one in (Daum and Huang, 2012a).

A generalisation of the incompressible flow was proposed by Daum and Huang in (Daum and Huang, 2010b), which is an important connection to the exact particle flow proposed in (Daum et al., 2010; Daum and Huang, 2011b). They were accompanied by the numerical analysis in (Daum and Huang, 2010c), which contains a comparison with the extended Kalman filter (EKF). The exact particle flow is different from the incompressible flow, where the non-zero divergence is allowed and is derived from the exact Fokker–Planck equation. The general solution of the exact particle flow $g_f(\underline{x}, \gamma)$ can be obtained as follows:

$$\begin{aligned} g_f(\underline{x}, \gamma) &= \frac{d\underline{x}}{d\gamma} \\ &= -C^{\#} \log f_L(\underline{x}) + \left(\mathbf{I} - C^{\#} C\right) \underline{c} \ , \end{aligned} \tag{15}$$

$$C = \left[\frac{\partial \log f_e(\underline{x}, \gamma)}{\partial \underline{x}} + \operatorname{tr}\left(\frac{\partial}{\partial \underline{x}}\right)\right] \ . \tag{16}$$

The operator C acts on a function ψ such that $C\psi = \left[\frac{\partial \log f_e(\underline{x},\gamma)}{\partial \underline{x}}\psi + \operatorname{tr}\left(\frac{\partial \psi}{\partial \underline{x}}\right)\right]$. If the two densities, $\log f_p(\underline{x})$ and $\log f_L(\underline{x})$, are Gaussian or belong to the exponential family, a closed-form solution, called the Gaussian flow, can be obtained as follows:

$$\frac{d\underline{x}}{d\gamma} = \mathbf{A}(\gamma)\,\underline{x} + \underline{b}(\gamma) \ , \tag{17}$$

$$\mathbf{A}(\gamma) = -\frac{1}{2}\mathbf{P}\boldsymbol{H}^\top\left(\gamma \boldsymbol{H}\mathbf{P}\boldsymbol{H}^\top + \mathbf{R}\right)^{-1}\boldsymbol{H} \ , \tag{18}$$

$$\underline{b}(\gamma) = (\mathbf{I} - 2\gamma\mathbf{A})\left[(\mathbf{I} + \gamma\mathbf{A})\,\mathbf{P}\boldsymbol{H}^\top\mathbf{R}^{-1}\underline{z} + \mathbf{A}\overline{\underline{x}}\right] \ , \tag{19}$$

where $\mathbf{P}$ is the covariance matrix of the samples (typically calculated as a sample covariance or obtained from other filters such as the EKF), $\boldsymbol{H}$ is the Jacobian matrix of the measurement model in (4) evaluated at the mean [2], $\mathbf{R}$ is the covariance matrix of the measurement noise, and $\overline{\underline{x}}$ is the mean of $\underline{x}$. For brevity, the argument (γ) is omitted from $\mathbf{A}(\gamma)$ on the right-hand side of (19). This solution of the particle flow is referred to as the exact flow Daum–Huang (EDH) filter in (Choi et al., 2011; Ding and Coates, 2012). The EDH filter will be considered for the comparative numerical study in Section 4. Further details can be found in (Daum et al., 2010), other solutions of the exact particle flow can be found in (Daum and Huang, 2010a), and the implementation of the EDH filter with applications can be found in (Choi et al., 2011).

Multiple solutions with various assumptions are given afterwards, and many of them in fact show the analogy to physics. In (Daum et al., 2011a), accompanied by the numerical simulations in (Daum et al., 2011b), it was shown that the derived PDE is similar to Coulomb's law, and in (Daum and Huang, 2012b), it was shown to be analogous to the Monge–Kantorovich transportation. Solutions assuming that the flow has small curvature (Daum and Huang, 2012c) and using the Fourier transform (Daum and Huang, 2013a) are also proposed. Another important advance in this branch is the non-zero diffusion (NZD) particle flow, also known as stochastic particle flow, proposed in (Daum and Huang, 2013d,b,e). In this approach, diffusion is no longer assumed to be zero during the evolution in artificial time, which makes the flow stochastic. The numerical solutions to mitigate the stiffness of the ODE of NZD particle flow are given in (Daum and Huang, 2014c), and the solutions and approximations of the covariance matrix of the diffusion are given in (Daum, 2016; Daum et al., 2016a). The analysis with numerical examples of these NZD particle flow filters is presented by Khan et al. in (Khan and Ulmke, 2014; Khan et al., 2017). Zero-curvature particle flow including geodesic particle flow (Daum and Huang, 2013f), upper-triangular Jacobian particle flow inspired by Knothe–Rosenblatt transport (Daum and Huang, 2013c), renormalisation group flow, which is a variant of NZD particle flow (Daum and Huang, 2014b), and further solutions for the flow and open questions (Daum and Huang, 2014a, 2015, 2016) were also proposed by Daum and Huang. While other stochastic particle flows exist, such as Gromov's flow (Daum et al., 2016b), they are omitted in this survey due to space limitations and will be discussed in future work.

Ding and Coates implemented the EDH filter for a target tracking application and proposed a further improvement in (Ding and Coates, 2012). In the EDH filter, $\mathbf{A}(\gamma)$ in (18) and $\underline{b}(\gamma)$ in (19) were computed only at the mean $\overline{\underline{x}}$. Alternatively, Ding and Coates proposed the local EDH (LEDH) filter, where $\mathbf{A}(\gamma)$ and $\underline{b}(\gamma)$ are computed for each particle individually by evaluating the Jacobian matrix $\boldsymbol{H}$ at each particle's location. The LEDH filter will be considered for the comparative numerical study in Section 4. Coates' group proposed more approaches that combine the EDH/LEDH with traditional PFs. Li et al. proposed an approach that combines particle flow with the auxiliary PF (APF) (Li et al., 2015b). In this study, the EDH was employed to sample auxiliary variables that define an importance sampling distribution in the APF framework. Another approach was proposed with traditional PFs in (Li et al., 2016), where EDH/LEDH serve as the proposal density followed by importance weighting, and it was named PFPF. Two variants of PFPF were proposed – a fast version with clustering to reduce the number of computations of (18) and (19) (Li and Coates, 2016), and an invertible variation of PFPF (Li and Coates, 2017). The latter, the invertible variation of PFPF with LEDH (PFPF-LEDH), will be considered for the comparative numerical study in Section 4. Similar but distinct approaches were proposed by Bunch and Godsill (Bunch and Godsill, 2013, 2016), where the particle flow is used not only to migrate the particles toward the posterior but also to update the importance weights.

We carefully selected the following papers, which contain the key approaches of this branch, for readers:

1) (Daum and Huang, 2009): The first paper that proposed the full form of the particle flow filter.
2) (Daum et al., 2010): EDH filter paper, which also includes the incompressible flow.
3) (Daum and Huang, 2013d): NZD particle flow (or stochastic particle flow), which allows the non-zero diffusion and generalises the EDH even further.
4) (Daum and Huang, 2013f): Zero curvature particle flow including geodesic particle flow.
5) (Li and Coates, 2017): Detailed information on the PFPF with applications.

[2] Italic $\boldsymbol{H}$ is used here to distinguish it from the Hessian $\mathbf{H}$ in (10).

3.3 Feedback Particle Filters Branch

This branch has been driven mainly by Mehta's group, and it utilises the control input, $\underline{u}_k$, in the time propagation step of (1) to migrate the particles. It is worth noting why this filter is included in the review, although the primary focus of this review is on the measurement update step, as mentioned in Section 2. It is mainly because the filters in this branch are derived in a continuous-time dynamic system, instead of a discrete-time dynamic system, and in this case, the control input can be considered in the same equation as the measurement update – this will be further explained later. The branch is named the *Feedback Particle Filters Branch*, since the algorithms are called feedback particle filters (FPFs) based on their analogy to a feedback controller structure.

Unlike the previous two branches, the FPF was first derived from a continuous-time stochastic partial differential equation (SPDE), the Zakai equation, and the model for the ith particle is defined as follows:

$$d\underline{\boldsymbol{x}}_t^i = \underline{a}_t\left(\underline{\boldsymbol{x}}_t^i\right)dt + d\underline{\boldsymbol{w}}_t^i + d\underline{u}_t^i \ , \tag{20}$$

where the measurement update is defined as a control problem by choosing the control input $\underline{u}_t^i$ in the optimal control form with a new measurement. In other words, the update step is considered in the same equation as the time propagation, and this is why we included this filter in the survey. Furthermore, by simply using an identity matrix for the time propagation, this filter can also be used without the propagation step. The idea of FPF was first introduced in (Yang et al., 2011b,a), and the complete study for the scalar FPF was proposed in (Yang et al., 2013). The explicit form of the optimal control $\underline{u}_t^i$ was derived in the paper as follows:

$$d\underline{\boldsymbol{x}}_t^i = \underline{a}_t\left(\underline{\boldsymbol{x}}_t^i\right)dt + d\underline{\boldsymbol{w}}_t^i + \underline{K}\left(\underline{\boldsymbol{x}}_t^i, t\right)d\underline{I}_t^i + \underline{\Omega}\left(\underline{\boldsymbol{x}}_t^i, t\right)dt \ , \tag{21}$$

where $\underline{K}\left(\underline{\boldsymbol{x}}_t^i, t\right)$ is a control gain, and the modified innovation $d\underline{I}_t^i$ and the Wong–Zakai correction term $\underline{\Omega}\left(\underline{\boldsymbol{x}}_t^i, t\right)$ are defined as follows:

$$d\underline{I}_t^i \overset{\text{def}}{=\!=} d\underline{z}_t - \frac{1}{2}\left(h\left(\underline{\boldsymbol{x}}_t^i\right) + \hat{h}_t\right)dt \ , \tag{22}$$

$$\underline{\Omega}\left(\underline{\boldsymbol{x}}_t^i, t\right) \overset{\text{def}}{=\!=} \frac{1}{2}\sigma_v^2 \underline{K}\left(\underline{\boldsymbol{x}}_t^i, t\right)\underline{K}'\left(\underline{\boldsymbol{x}}_t^i, t\right) \ , \tag{23}$$

$$\underline{K}'\left(\underline{\boldsymbol{x}}_t^i, t\right) = \frac{\partial \underline{K}(\underline{\boldsymbol{x}}, t)}{\partial \underline{\boldsymbol{x}}} \ , \tag{24}$$

where $\hat{h}_t$ is the expected value of $h\left(\underline{\boldsymbol{x}}_t^i\right)$ given the measurements, which has been approximated for numerical implementation using N samples as follows:

$$\hat{h}_t \approx \hat{h}_t^{(N)} := \frac{1}{N}\sum_{i=1}^{N} h\left(\underline{\boldsymbol{x}}_t^i\right) \ . \tag{25}$$

The control gain $\underline{K}\left(\underline{\boldsymbol{x}}_t^i, t\right)$ can be calculated by solving the Poisson equation (Yang et al., 2013), and it can be approximated using a Galerkin numerical method with the basis functions from the polynomial family, $\{\underline{x}, \underline{x}^2, \cdots, \underline{x}^M\}$. The constant-gain approximation, a special case of a Galerkin numerical method when $M = 1$, in the linear Gaussian case can be denoted as follows:

$$\begin{aligned}\mathbb{E}\left[\underline{K}_t\left(\underline{\boldsymbol{x}}_t\right)|\underline{z}_t\right] &= \int_{\mathbb{R}_d}\left(h\left(\underline{\boldsymbol{x}}\right) - \hat{h}_t\right)\underline{\boldsymbol{x}} f_t^e\left(\underline{\boldsymbol{x}}\right)d\underline{\boldsymbol{x}} \\ &\approx \frac{1}{N}\sum_{i=1}^{N}\left(h\left(\underline{\boldsymbol{x}}_t^i\right) - \hat{h}_t^{(N)}\right)\underline{\boldsymbol{x}}_t^i \ .\end{aligned} \tag{26}$$

However, the Galerkin approximation can exhibit numerical issues related to the Gibbs phenomenon and this motivated a data-driven basis function selection (Berntorp and Grover, 2016, 2018) and a basis-free diffusion map-based approach (Taghvaei and Mehta, 2016; Taghvaei et al., 2017, 2020). It is worth noting that the control gain $\underline{K}\left(\underline{\boldsymbol{x}}_t^i, t\right)$ is equivalent to the Kalman gain in the linear Gaussian case, and the authors explicitly state, "The linear Gaussian FPF is identical to the square-root form of the ensemble Kalman filter" (Taghvaei et al., 2020, p. 3). Further details of the FPF can be found in (Yang et al., 2013). The FPF with constant-gain (FPF-CG) and the FPF with diffusion map-based gain (FPF-DM) will be considered for the comparative numerical study in Section 4, and further discussion will be provided in Section 5.

A multivariate FPF was proposed in (Yang et al., 2012), and details are provided in (Yang et al., 2016), while a comparative study and applications are presented in (Tilton et al., 2013; Berntorp, 2015).

We carefully selected the following papers, which contain the key approaches of this branch, for readers:

1) (Yang et al., 2013): Complete version of the FPF.
2) (Yang et al., 2016): Complete version of the multivariate FPF with details.
3) (Taghvaei et al., 2020): Diffusion map-based gain FPF with multiple numerical examples.

4. COMPARATIVE NUMERICAL SIMULATION

In order to analyse the characteristics of each branch and compare their performance, a comparative numerical simulation is presented. The comparison focuses on the qualitative performance of the filters, i.e., how well each algorithm forms the posterior density in two-dimensional space given the prior density and the measurement. Note that no direct comparison of computational cost is performed in this simulation, since the algorithms are currently implemented in different programming languages. Performing such a comparison, after reimplementing them in a unified programming language, is left for future work.

4.1 Simulation Setup

To illustrate and qualitatively compare the performance of the introduced filters from the previous sections, we consider a simple two-dimensional range-only example, as shown in Fig. 2.

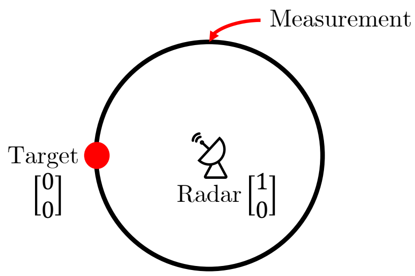

Fig. 2. **A two-dimensional range-only example.** A radar at $[1, 0]^\top$ estimates the position of a target at $[0, 0]^\top$ from a range-only measurement.

This simple and powerful example illustrates how well the filters can approximate the true posterior density with two-dimensional samples. A radar placed at $[1,0]^\top$ measures the position of a target placed at $[0,0]^\top$ using a range-only measurement corrupted by zero-mean Gaussian noise with $\sigma_v = 0.1$, $\boldsymbol{v} \sim f_{\boldsymbol{v}}(\boldsymbol{v}) = \mathcal{N}(\boldsymbol{v}; 0, \sigma_v)$. The prior density is a Gaussian distribution, $f_p(\underline{\boldsymbol{x}}) = \mathcal{N}\left(\underline{\boldsymbol{x}}; \underline{0}, \mathbf{I}\right)$. The measurement function is defined as follows:

$$h\left(\underline{\boldsymbol{x}}\right) = \sqrt{\left(\boldsymbol{x}_1 - 1\right)^2 + \boldsymbol{x}_2^2} + \boldsymbol{v} \ . \tag{27}$$

One measurement update step without time propagation is considered. For the FPF, where the time propagation and measurement update are performed simultaneously using (21), an identity matrix is used for the propagation step with zero process noise. Based on this scenario and the Gaussian prior density, we can expect the posterior density to be ring-shaped, with denser samples around the target location at $[0,0]^\top$, as shown in Fig. 3.

Fig. 3. **Posterior density after one measurement update step.** The measurement update produces a ring-shaped posterior density with higher likelihood around the target location.

The following algorithms are considered for comparison: 1) PBFs branch – NF, 2) DHFs branch – EDH, LEDH, and PFPF-LEDH, and 3) FPFs branch – FPF-CG and FPF-DM. In the implementation, the number of artificial time steps within one particle flow is determined by the ODE solver in the case of the NF, and is set to 29 exponential steps for EDH, LEDH, and PFPF-LEDH. For the FPFs, the continuous-time measurement update is approximated by numerical discretisation with 100 time steps. For DHFs, the EKF is utilised in parallel to calculate the covariance of the samples in (18) and (19). The comparison of the filter implementations is summarised in Table 1. Two prior sample sets are considered in the simulation: 1) deterministic sample set, and 2) random sample set.

Table 1. A summary of the compared filters

Branch	PBFs	DHFs	FPFs
Filters	NF	EDH, LEDH, PFPF-LEDH	FPF-CG, FPF-DM
No. of steps	ODE solver	29 steps	100 steps
Programming language	Julia	MATLAB	Python

4.2 Deterministic Prior Sample set

A deterministic sample set is drawn from the Gaussian distribution using LCD, based on the method proposed in (Hanebeck and Klumpp, 2008). This allows the prior sample set to be well distributed in the state space, even with a small number of samples. A total of 100 samples are drawn deterministically, and the same sample set is used as the prior for all tested filters. The final step of the particle flow for each filter is shown in Fig. 4.

The results suggest that the NF performs best with the deterministic sample set, and other filters, including LEDH, PFPF-LEDH, and FPF-DM, can also form the posterior density well. The LEDH and FPF-DM show slightly biased results compared to the NF or PFPF-LEDH. The PFPF-LEDH exhibits smaller variance in the sample distribution compared to the LEDH, which is due to the additional importance weighting step within PFPF. On the other hand, EDH and FPF-CG fail to form the posterior distribution. This is mainly caused by their formulation: computation of (17) only at the mean for EDH, and the constant-gain in (26) for FPF-CG. Further details will be discussed in Section 5.

4.3 Random Prior Sample set

A total of 100 random samples are drawn from the Gaussian distribution, and the same sample set is used as the prior for all tested filters. The final step of the particle flow for each filter is shown in Fig. 5.

The results suggest that the LEDH performs best with the random sample set, while the PFPF-LEDH exhibits smaller variance in the sample distribution, again due to the importance sampling, and the FPF-DM shows a biased result similar to the previous example. The NF is not able to form the expected posterior density with the random prior sample set, which is due to its inherent characteristic of using deterministic sampling within the algorithm. In addition, EDH and FPF-CG again fail to form the posterior distribution.

4.4 Multi-modal Prior Density

An additional numerical simulation with a multi-modal prior density is performed. The same problem setup as in the previous example is considered, but the prior sample set is deterministically drawn from a GM distribution, $f_p(\underline{\boldsymbol{x}}) = \mathcal{N}\left(\underline{\boldsymbol{x}}; [-20,0]^\top, \mathbf{I}\right) + \mathcal{N}\left(\underline{\boldsymbol{x}}; [-10,0]^\top, \mathbf{I}\right)$. This represents a scenario in which the overlap between the prior and the likelihood is very small or nonexistent – where the particle degeneracy issue can be significant with a multi-modal prior density. A total of 200 samples are drawn deterministically, and the same sample set is used as the prior for all tested filters. The final step of the particle flow for each filter is shown in Fig. 6.

The results suggest that the NF performs best with the GM sample set. A similar trend is observed for the other filters, consistent with the previous examples. In addition, the NF shows the samples in one cluster, whereas all other filters clearly show two separate clusters, indicating that the DHFs are independent of the prior samples. The FPFs are not able to perform the filtering in this example.

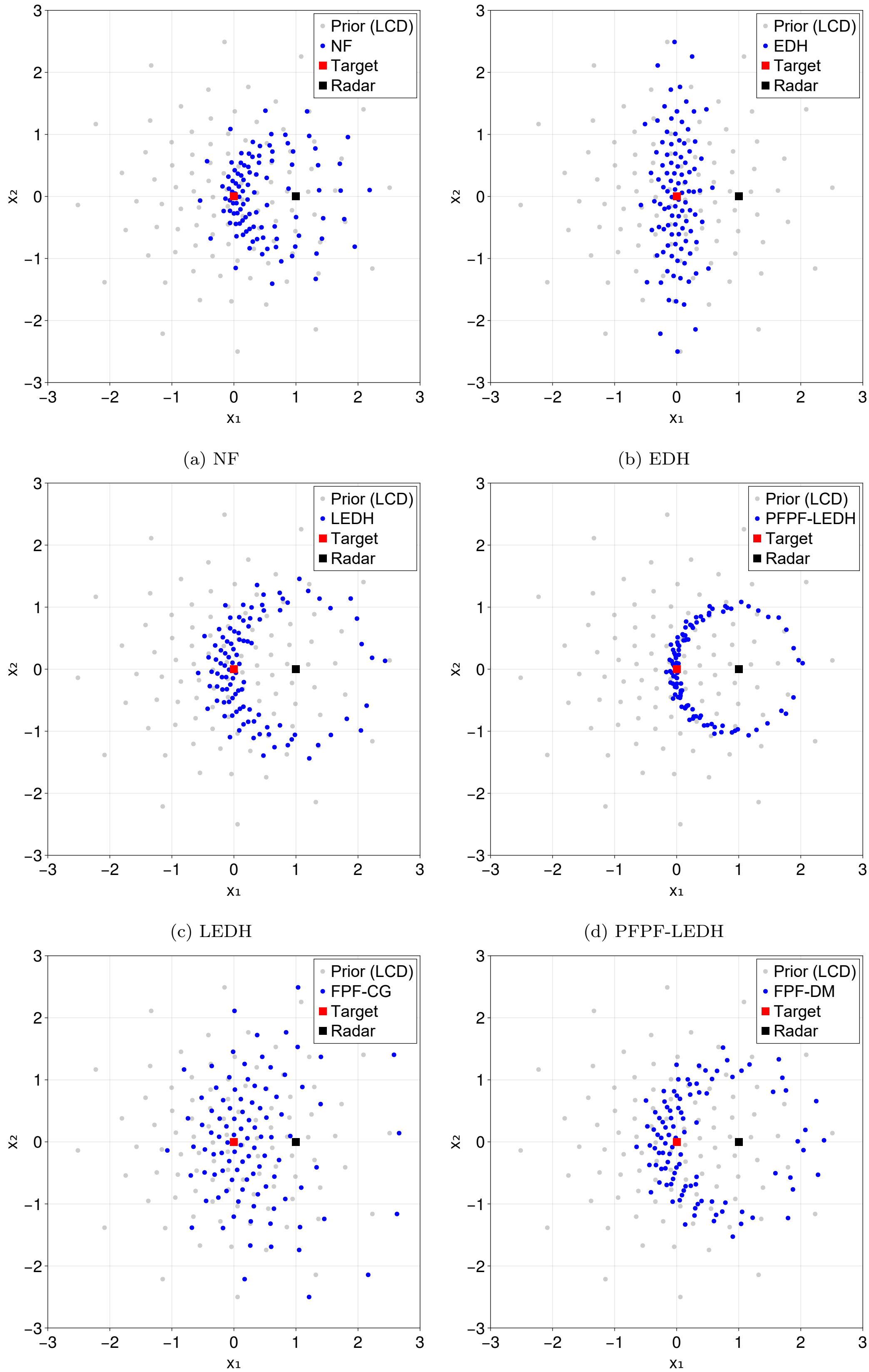

(a) NF (b) EDH (c) LEDH (d) PFPF-LEDH (e) FPF-CG (f) FPF-DM

Fig. 4. **Results of the simulation at $\gamma = 1$ with a deterministic prior sample set.** The final state of the particle flow for each filter is shown. Note that all samples are unweighted.

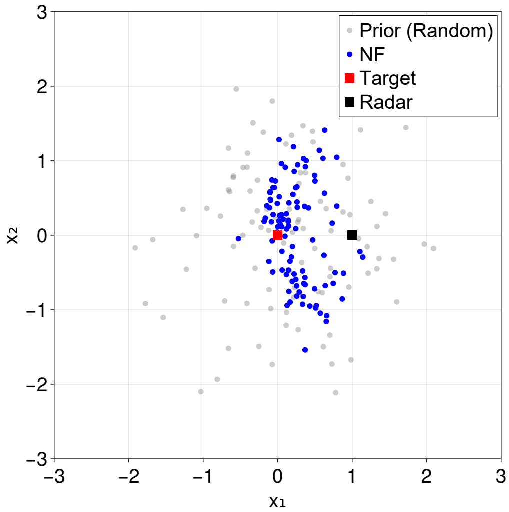

(a) NF

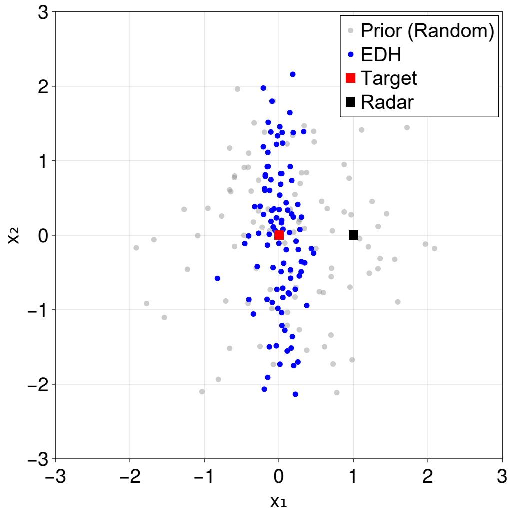

(b) EDH

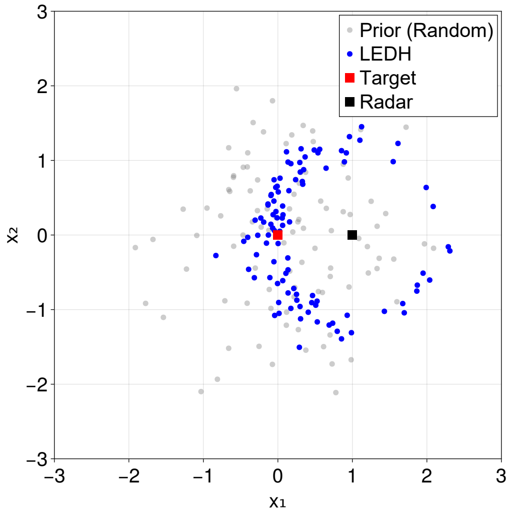

(c) LEDH

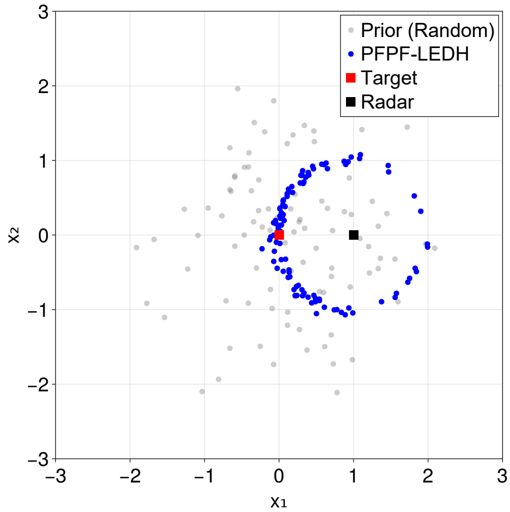

(d) PFPF-LEDH

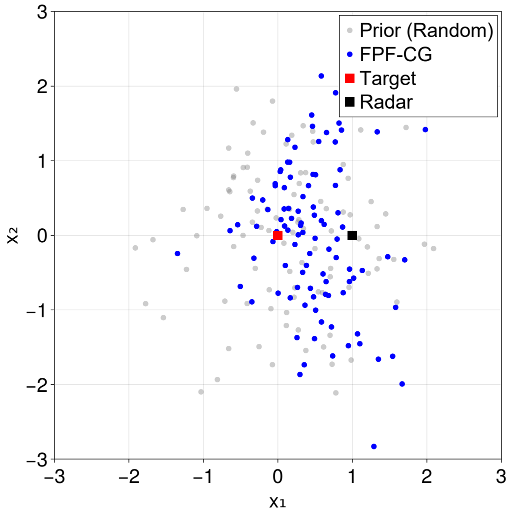

(e) FPF-CG

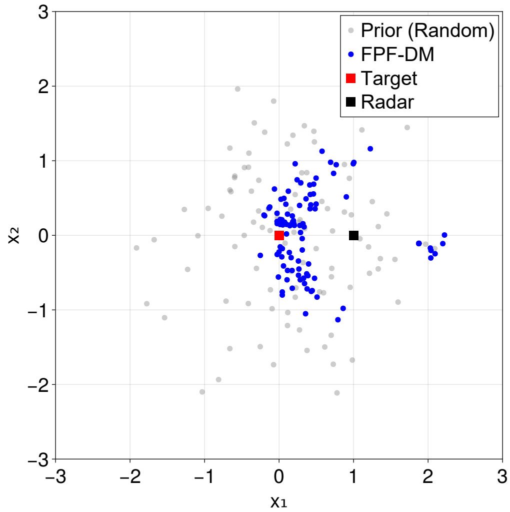

(f) FPF-DM

Fig. 5. **Results of the simulation at $\gamma = 1$ with a random prior sample set.** The final state of the particle flow for each filter is shown. Note that all samples are unweighted.

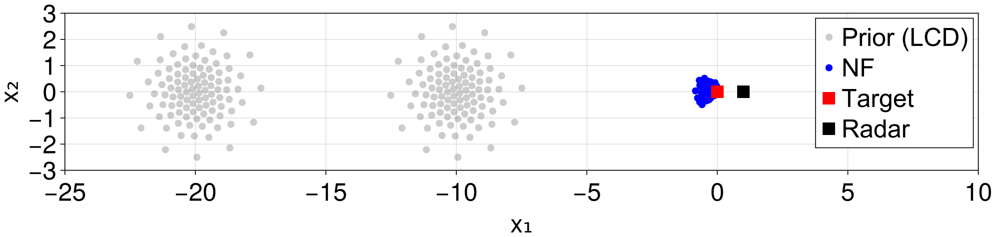

(a) NF

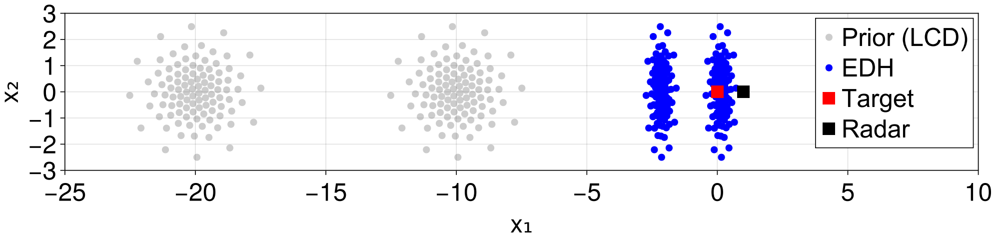

(b) EDH

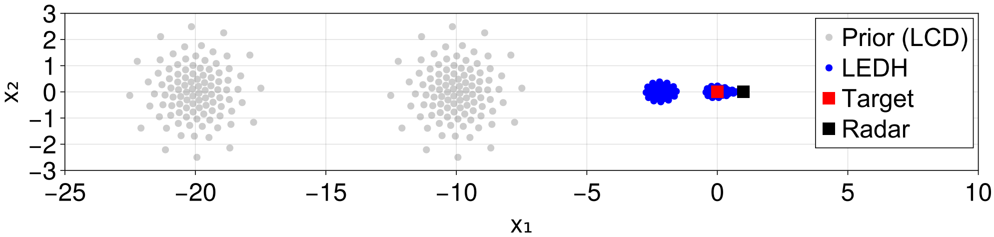

(c) LEDH

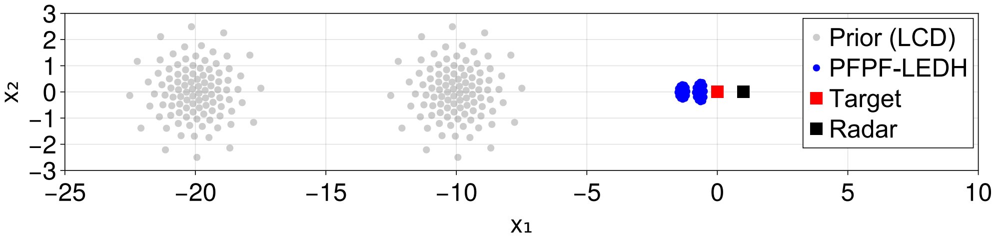

(d) PFPF-LEDH

Fig. 6. **Results of the simulation at $\gamma = 1$ with a deterministic GM prior sample set.** The final state of the particle flow for each filter is shown. Note that all samples are unweighted.

5. DISCUSSION

The NF from the PBFs branch shows good performance with both the deterministic prior sample set and the deterministic GM prior sample set. Its inherent continuous flow formulation, based on deterministic sampling, makes the NF dependent on the specific prior sample set. However, the NF does not actually consider global information about the prior density, such as the sample covariance. Because of this lack of global context, its performance with a random sample set can be degraded, as it relies entirely on the initial distribution of the samples.

The EDH from the DHFs branch shows a critical issue in the previous examples: it linearises and computes the coefficients in (17) only at the mean. This results in nearly zero flow along the x_2-axis and widely spread samples. The LEDH, as expected, overcomes this issue through local linearisation and calculation of the coefficients in (17). The PFPF-LEDH produces smaller sample variance compared to the LEDH, which serves as the baseline for the PFPF, and this is due to the additional importance weighting in PFPF. The reason why filters in the DHFs branch perform well with random samples but struggle with a GM prior is that their flow relies on global information, specifically the sample covariance calculated via the EKF. This dependence on global statistics makes the flow independent of the specific prior sample locations but limits performance when dealing with multi-modal densities.

The FPF-CG from the FPFs branch also shows a limitation in the gain computation in (26), as the terms may cancel each other out, resulting in a nearly zero gain. For this reason, the samples of FPF-CG are more widely spread at the end of the iteration. Another issue, not mentioned previously, is that the FPF exhibits wobbling during the iteration. This occurs because the algorithm calculates the solution of the Poisson equation to obtain a control gain at every discretised time step without any temporal smoothing.

6. CONCLUSION

Particle flow-based filters are an effective alternative for mitigating the particle degeneracy issue commonly encountered in traditional PFs. We surveyed a bulk of studies on particle flow-based filters and introduced the key works from the "galaxy" of them. In addition, we tested the main filters from three branches – progressive Bayesian filters (PBFs) branch, Daum–Huang filters (DHFs) branch, and feedback particle filters (FPFs) branch – using a two-dimensional range-only measurement estimation example. The results suggest that the Newton-flow (NF) is a powerful tool with deterministic prior sample sets, and even when the prior follows a GM distribution. In addition, the NF exhibits greater homogeneity of the posterior samples relative to other approaches. The local exact Daum–Huang (LEDH) filter also showed good performance, independent of the prior samples, although limitations due to the accompanied extended Kalman filter (EKF) were noted. Limitations of the feedback particle filter (FPF), particularly the constant-gain variant, were also discussed.

More recent works on particle flow-based filters have evolved in two directions: 1) Gaussian mixture models to represent the densities, and 2) combinations with recently developed machine learning techniques. The details of these are omitted in this version due to space limitations. An extended version will provide more recent advances in particle flow-based filters, including optimal transport (OT) and variational inference (VI) approaches. Furthermore, deeper numerical simulations covering high-dimensional examples will be provided. This future research will also include quantitative analyses and computational cost comparisons against newer developments in stochastic particle flow, such as Gromov's flow.

ACKNOWLEDGEMENTS

The authors gratefully acknowledge Professor Mark Coates and Professor Amir Taghvaei for providing source code and for their valuable discussions.

REFERENCES

Berntorp, K. (2015). Feedback particle filter: Application and evaluation. In *2015 18th International Conference on Information Fusion (Fusion)*, 1633–1640.

Berntorp, K. and Grover, P. (2016). Data-driven gain computation in the feedback particle filter. In *2016 American Control Conference (ACC)*, 2711–2716.

Berntorp, K. and Grover, P. (2018). Feedback particle filter with data-driven gain-function approximation. *IEEE Transactions on Aerospace and Electronic Systems*, 54(5), 2118–2130.

Bunch, P. and Godsill, S. (2013). Particle filtering with progressive Gaussian approximations to the optimal importance density. In *2013 5th IEEE International Workshop on Computational Advances in Multi-Sensor Adaptive Processing (CAMSAP)*, 360–363.

Bunch, P. and Godsill, S. (2016). Approximations of the optimal importance density using Gaussian particle flow importance sampling. *Journal of the American Statistical Association*, 111(514), 748–762.

Chen, L. and Mehra, R.K. (2010). A study of nonlinear filters with particle flow induced by log-homotopy. In I. Kadar (ed.), *Signal Processing, Sensor Fusion, and Target Recognition XIX*, volume 7697, 769706. International Society for Optics and Photonics, SPIE.

Chlebek, C., Steinbring, J., and Hanebeck, U.D. (2016). Progressive Gaussian filter using importance sampling and particle flow. In *2016 19th International Conference on Information Fusion (FUSION)*, 2043–2049.

Choi, S., Willett, P., Daum, F., and Huang, J. (2011). Discussion and application of the homotopy filter. In I. Kadar (ed.), *Signal Processing, Sensor Fusion, and Target Recognition XX*, volume 8050, 805021. International Society for Optics and Photonics, SPIE.

Daum, F. (2016). Seven dubious methods to compute optimal Q for Bayesian stochastic particle flow. In *2016 19th International Conference on Information Fusion (FUSION)*, 2237–2244.

Daum, F. and Huang, J. (2007). Nonlinear filters with log-homotopy. In O.E. Drummond and R.D. Teichgraeber (eds.), *Signal and Data Processing of Small Targets 2007*, volume 6699, 669918. International Society for Optics and Photonics, SPIE.

Daum, F. and Huang, J. (2008). Particle flow for nonlinear filters with log-homotopy. In O.E. Drummond (ed.), *Signal and Data Processing of Small Targets 2008*, volume 6969, 696918. International Society for Optics and Photonics, SPIE.

Daum, F. and Huang, J. (2010a). Exact particle flow for nonlinear filters: Seventeen dubious solutions to a first order linear underdetermined PDE. In *2010 Conference Record of the Forty Fourth Asilomar Conference on Signals, Systems and Computers*, 64–71.

Daum, F. and Huang, J. (2010b). Generalized particle flow for nonlinear filters. In O.E. Drummond (ed.), *Signal and Data Processing of Small Targets 2010*, volume 7698, 76980I. International Society for Optics and Photonics, SPIE.

Daum, F. and Huang, J. (2010c). Numerical experiments for nonlinear filters with exact particle flow induced by log-homotopy. In O.E. Drummond (ed.), *Signal and Data Processing of Small Targets 2010*, volume 7698, 769816. International Society for Optics and Photonics, SPIE.

Daum, F. and Huang, J. (2011a). Particle degeneracy: root cause and solution. In I. Kadar (ed.), *Signal Processing, Sensor Fusion, and Target Recognition XX*, volume 8050, 80500W. International Society for Optics and Photonics, SPIE.

Daum, F. and Huang, J. (2011b). Particle flow for nonlinear filters. In *2011 IEEE International Conference on Acoustics, Speech and Signal Processing (ICASSP)*, 5920–5923.

Daum, F. and Huang, J. (2012a). Friendly rebuttal to Chen and Mehra: incompressible particle flow for nonlinear filters. In I. Kadar (ed.), *Signal Processing, Sensor Fusion, and Target Recognition XXI*, volume 8392, 839210. International Society for Optics and Photonics, SPIE.

Daum, F. and Huang, J. (2012b). Particle flow and Monge-Kantorovich transport. In *2012 15th International Conference on Information Fusion*, 135–142.

Daum, F. and Huang, J. (2012c). Small curvature particle flow for nonlinear filters. In O.E. Drummond and R.D. Teichgraeber (eds.), *Signal and Data Processing of*

Small Targets 2012, volume 8393, 83930A. International Society for Optics and Photonics, SPIE.

Daum, F. and Huang, J. (2013a). Fourier transform particle flow for nonlinear filters. In I. Kadar (ed.), *Signal Processing, Sensor Fusion, and Target Recognition XXII*, volume 8745, 87450R. International Society for Optics and Photonics, SPIE.

Daum, F. and Huang, J. (2013b). Particle flow for nonlinear filters, Bayesian decisions and transport. In *Proceedings of the 16th International Conference on Information Fusion*, 1072–1079.

Daum, F. and Huang, J. (2013c). Particle flow inspired by Knothe-Rosenblatt transport for nonlinear filters. In I. Kadar (ed.), *Signal Processing, Sensor Fusion, and Target Recognition XXII*, volume 8745, 87450O. International Society for Optics and Photonics, SPIE.

Daum, F. and Huang, J. (2013d). Particle flow with non-zero diffusion for nonlinear filters. In I. Kadar (ed.), *Signal Processing, Sensor Fusion, and Target Recognition XXII*, volume 8745, 87450P. International Society for Optics and Photonics, SPIE.

Daum, F. and Huang, J. (2013e). Particle flow with non-zero diffusion for nonlinear filters, Bayesian decisions and transport. In O.E. Drummond and R.D. Teichgraeber (eds.), *Signal and Data Processing of Small Targets 2013*, volume 8857, 88570A. International Society for Optics and Photonics, SPIE.

Daum, F. and Huang, J. (2013f). Zero curvature particle flow for nonlinear filters. In I. Kadar (ed.), *Signal Processing, Sensor Fusion, and Target Recognition XXII*, volume 8745, 87450Q. International Society for Optics and Photonics, SPIE.

Daum, F. and Huang, J. (2014a). How to avoid normalization of particle flow for nonlinear filters, Bayesian decisions, and transport. In O.E. Drummond (ed.), *Signal and Data Processing of Small Targets 2014*, volume 9092, 90920B. International Society for Optics and Photonics, SPIE.

Daum, F. and Huang, J. (2014b). Renormalization group flow and other ideas inspired by physics for nonlinear filters, Bayesian decisions, and transport. In I. Kadar (ed.), *Signal Processing, Sensor/Information Fusion, and Target Recognition XXIII*, volume 9091, 90910I. International Society for Optics and Photonics, SPIE.

Daum, F. and Huang, J. (2014c). Seven dubious methods to mitigate stiffness in particle flow with non-zero diffusion for nonlinear filters, Bayesian decisions, and transport. In O.E. Drummond (ed.), *Signal and Data Processing of Small Targets 2014*, volume 9092, 90920C. International Society for Optics and Photonics, SPIE.

Daum, F. and Huang, J. (2015). A baker's dozen of new particle flows for nonlinear filters, Bayesian decisions and transport. In I. Kadar (ed.), *Signal Processing, Sensor/Information Fusion, and Target Recognition XXIV*, volume 9474, 94740J. International Society for Optics and Photonics, SPIE.

Daum, F. and Huang, J. (2016). A plethora of open problems in particle flow research for nonlinear filters, Bayesian decisions, Bayesian learning, and transport. In I. Kadar (ed.), *Signal Processing, Sensor/Information Fusion, and Target Recognition XXV*, volume 9842, 98420I. International Society for Optics and Photonics, SPIE.

Daum, F., Huang, J., Krichman, M., and Kohen, T. (2009a). Seventeen dubious methods to approximate the gradient for nonlinear filters with particle flow. In O.E. Drummond and R.D. Teichgraeber (eds.), *Signal and Data Processing of Small Targets 2009*, volume 7445, 74450V. International Society for Optics and Photonics, SPIE.

Daum, F., Huang, J., and Noushin, A. (2010). Exact particle flow for nonlinear filters. In I. Kadar (ed.), *Signal Processing, Sensor Fusion, and Target Recognition XIX*, volume 7697, 769704. International Society for Optics and Photonics, SPIE.

Daum, F., Huang, J., and Noushin, A. (2011a). Coulomb's law particle flow for nonlinear filters. In O.E. Drummond (ed.), *Signal and Data Processing of Small Targets 2011*, volume 8137, 81370B. International Society for Optics and Photonics, SPIE.

Daum, F., Huang, J., and Noushin, A. (2011b). Numerical experiments for Coulomb's law particle flow for nonlinear filters. In O.E. Drummond (ed.), *Signal and Data Processing of Small Targets 2011*, volume 8137, 81370E. International Society for Optics and Photonics, SPIE.

Daum, F., Huang, J., and Noushin, A. (2016a). Gromov's method for Bayesian stochastic particle flow: A simple exact formula for Q. In *2016 IEEE International Conference on Multisensor Fusion and Integration for Intelligent Systems (MFI)*, 540–545.

Daum, F., Huang, J., and Noushin, A. (2016b). Gromov's method for Bayesian stochastic particle flow: A simple exact formula for Q. In *2016 IEEE International Conference on Multisensor Fusion and Integration for Intelligent Systems (MFI)*, 540–545.

Daum, F. and Huang, J. (2009). Nonlinear filters with particle flow induced by log-homotopy. In I. Kadar (ed.), *Signal Processing, Sensor Fusion, and Target Recognition XVIII*, volume 7336, 733603. International Society for Optics and Photonics, SPIE.

Daum, F., Huang, J., Noushin, A.J., and Krichman, M. (2009b). Gradient estimation for particle flow induced by log-homotopy for nonlinear filters. In I. Kadar (ed.), *Signal Processing, Sensor Fusion, and Target Recognition XVIII*, volume 7336, 733602. International Society for Optics and Photonics, SPIE.

Ding, T. and Coates, M.J. (2012). Implementation of the Daum-Huang exact-flow particle filter. In *2012 IEEE Statistical Signal Processing Workshop (SSP)*, 257–260.

Hagmar, J., Jirstrand, M., Svensson, L., and Morelande, M. (2011). Optimal parameterization of posterior densities using homotopy. In *14th International Conference on Information Fusion*, 1–8.

Hanebeck, U. and Feiermann, O. (2003). Progressive Bayesian estimation for nonlinear discrete-time systems:the filter step for scalar measurements and multidimensional states. In *42nd IEEE International Conference on Decision and Control (IEEE Cat. No.03CH37475)*, volume 5, 5366–5371 Vol.5.

Hanebeck, U.D. (2013). PGF 42: Progressive Gaussian filtering with a twist. In *Proceedings of the 16th International Conference on Information Fusion*, 1103–1110.

Hanebeck, U.D. (2025). Newton-flow particle filters based on generalized Cramér distance. *arXiv preprint arXiv:2509.00182*.

Hanebeck, U.D., Briechle, K., and Rauh, A. (2003). Progressive Bayes: a new framework for nonlinear state estimation. In B.V. Dasarathy (ed.), *Multisensor, Multisource Information Fusion: Architectures, Algorithms, and Applications 2003*, volume 5099, 256 – 267. International Society for Optics and Photonics, SPIE.

Hanebeck, U.D., Huber, M.F., and Klumpp, V. (2009). Dirac mixture approximation of multivariate Gaussian densities. In *Proceedings of the 48h IEEE Conference on Decision and Control (CDC) held jointly with 2009 28th Chinese Control Conference*, 3851–3858.

Hanebeck, U.D. and Klumpp, V. (2008). Localized cumulative distributions and a multivariate generalization of the Cramér-von Mises distance. In *2008 IEEE International Conference on Multisensor Fusion and Integration for Intelligent Systems*, 33–39.

Hanebeck, U.D. and Pander, M. (2016). Progressive Bayesian estimation with deterministic particles. In *2016 19th International Conference on Information Fusion (FUSION)*, 2028–2034.

Hanebeck, U.D. and Steinbring, J. (2012). Progressive Gaussian filtering based on Dirac mixture approximations. In *2012 15th International Conference on Information Fusion*, 1697–1704.

Khan, M.A. and Ulmke, M. (2014). Non-linear and non-Gaussian state estimation using log-homotopy based particle flow filters. In *2014 Sensor Data Fusion: Trends, Solutions, Applications (SDF)*, 1–6.

Khan, M.A., Ulmke, M., and Koch, W. (2017). Analysis of log-homotopy based particle flow filters. *Journal of Advances in Information Fusion (JAIF)*, 12(1).

Kim, S., Moon, S., Petrunin, I., Shin, H.S., and Khattak, S. (2025a). Autonomous robotic radio source localization via a novel Gaussian mixture filtering approach. In *2025 28th International Conference on Information Fusion (FUSION)*, 1–8.

Kim, S., Petrunin, I., and Shin, H.S. (2022). A review of Kalman filter with artificial intelligence techniques. *2022 Integrated Communication, Navigation and Surveillance Conference (ICNS)*, 1–12.

Kim, S., Petrunin, I., and Shin, H.S. (2025b). A review of Bayes filters with machine learning techniques and their applications. *Information Fusion*, 114, 102707.

Kim, S., Sun, M., Petrunin, I., and Shin, H.S. (2026). Dbscan-based particle Gaussian mixture filters. *Digital Signal Processing*, 168, 105546.

Kotecha, J.H. and Djurić, P.M. (2003). Gaussian sum particle filtering. *IEEE Transactions on Signal Processing*, 51(10), 2602.

Kuptametee, C. and Aunsri, N. (2022). A review of resampling techniques in particle filtering framework. *Measurement*, 193, 110836.

Li, T., Bolic, M., and Djuric, P.M. (2015a). Resampling methods for particle filtering: Classification, implementation, and strategies. *IEEE Signal Processing Magazine*, 32(3), 70–86.

Li, T., Sun, S., Sattar, T.P., and Corchado, J.M. (2014). Fight sample degeneracy and impoverishment in particle filters: A review of intelligent approaches. *Expert Systems with Applications*, 41(8), 3944–3954.

Li, Y. and Coates, M. (2016). Fast particle flow particle filters via clustering. In *2016 19th International Conference on Information Fusion (FUSION)*, 2022–2027.

Li, Y. and Coates, M. (2017). Particle filtering with invertible particle flow. *IEEE Transactions on Signal Processing*, 65(15), 4102–4116.

Li, Y., Zhao, L., and Coates, M. (2015b). Particle flow auxiliary particle filter. In *2015 IEEE 6th International Workshop on Computational Advances in Multi-Sensor Adaptive Processing (CAMSAP)*, 157–160.

Li, Y., Zhao, L., and Coates, M. (2016). Particle flow for particle filtering. In *2016 IEEE International Conference on Acoustics, Speech and Signal Processing (ICASSP)*, 3979–3983.

Oudjane, N. and Musso, C. (2000). Progressive correction for regularized particle filters. In *Proceedings of the Third International Conference on Information Fusion*, volume 2, THB2/10–THB2/17 vol.2.

Psiaki, M.L. (2015). Gaussian mixture nonlinear filtering with resampling for mixand narrowing. *IEEE Transactions on Signal Processing*, 64(21), 5499–5512.

Raihan, D. and Chakravorty, S. (2018). Particle Gaussian mixture filters-i. *Automatica*, 98, 331–340.

Ruoff, P., Krauthausen, P., and Hanebeck, U.D. (2011). Progressive correction for deterministic Dirac mixture approximations. In *14th International Conference on Information Fusion*, 1–8.

Steinbring, J. and Hanebeck, U.D. (2014). Progressive Gaussian filtering using explicit likelihoods. In *17th International Conference on Information Fusion (FUSION)*, 1–8.

Taghvaei, A. and Mehta, P.G. (2016). Gain function approximation in the feedback particle filter. In *2016 IEEE 55th Conference on Decision and Control (CDC)*, 5446–5452.

Taghvaei, A., Mehta, P.G., and Meyn, S.P. (2017). Error estimates for the kernel gain function approximation in the feedback particle filter. In *2017 American Control Conference (ACC)*, 4576–4582.

Taghvaei, A., Mehta, P.G., and Meyn, S.P. (2020). Diffusion map-based algorithm for gain function approximation in the feedback particle filter. *SIAM/ASA Journal on Uncertainty Quantification*, 8(3), 1090–1117.

Tilton, A.K., Ghiotto, S., and Mehta, P.G. (2013). A comparative study of nonlinear filtering techniques. In *Proceedings of the 16th International Conference on Information Fusion*, 1827–1834.

Yang, T., Laugesen, R.S., Mehta, P.G., and Meyn, S.P. (2012). Multivariable feedback particle filter. In *2012 IEEE 51st IEEE Conference on Decision and Control (CDC)*, 4063–4070.

Yang, T., Laugesen, R.S., Mehta, P.G., and Meyn, S.P. (2016). Multivariable feedback particle filter. *Automatica*, 71, 10–23.

Yang, T., Mehta, P.G., and Meyn, S.P. (2011a). Feedback particle filter with mean-field coupling. In *2011 50th IEEE Conference on Decision and Control and European Control Conference*, 7909–7916.

Yang, T., Mehta, P.G., and Meyn, S.P. (2011b). A mean-field control-oriented approach to particle filtering. In *Proceedings of the 2011 American Control Conference*, 2037–2043.

Yang, T., Mehta, P.G., and Meyn, S.P. (2013). Feedback particle filter. *IEEE Transactions on Automatic Control*, 58(10), 2465–2480.